

**UCC Library and UCC researchers have made this item openly available.
Please [let us know](#) how this has helped you. Thanks!**

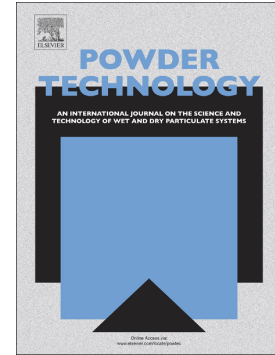
Title	The application of percolation threshold theory to predict compaction behaviour of pharmaceutical powder blends
Author(s)	Queiroz, Ana Luiza P.; Faisal, Waleed; Devine, Ken; Garvie-Cook, Hazel; Vucen, Sonja; Crean, Abina M.
Publication date	2019-05-13
Original citation	Queiroz, A. P. L., Faisal, W., Devine, K., Garvie-Cook, H., Vucen, S., and Crean, A. M. (2019) 'The application of percolation threshold theory to predict compaction behaviour of pharmaceutical powder blends', Powder Technology, 354, pp. 188-198. doi: 10.1016/j.powtec.2019.05.027
Type of publication	Article (peer-reviewed)
Link to publisher's version	http://www.sciencedirect.com/science/article/pii/S0032591019303675 http://dx.doi.org/10.1016/j.powtec.2019.05.027 Access to the full text of the published version may require a subscription.
Rights	© 2019 Elsevier B. V. All rights reserved. This manuscript version is made available under the CC BY-NC-ND 4.0 license.
Embargo information	Access to this article is restricted until 24 months after publication by request of the publisher
Embargo lift date	2021-05-13
Item downloaded from	http://hdl.handle.net/10468/9875

Downloaded on 2021-11-27T14:18:02Z

Accepted Manuscript

The application of percolation threshold theory to predict compaction behaviour of pharmaceutical powder blends

Ana Luiza P. Queiroz, Waleed Faisal, Ken Devine, Hazel Garvie-Cook, Sonja Vucen, Abina M. Crean



PII: S0032-5910(19)30367-5
DOI: <https://doi.org/10.1016/j.powtec.2019.05.027>
Reference: PTEC 14345
To appear in: *Powder Technology*
Received date: 15 January 2019
Revised date: 7 May 2019
Accepted date: 11 May 2019

Please cite this article as: A.L.P. Queiroz, W. Faisal, K. Devine, et al., The application of percolation threshold theory to predict compaction behaviour of pharmaceutical powder blends, Powder Technology, <https://doi.org/10.1016/j.powtec.2019.05.027>

This is a PDF file of an unedited manuscript that has been accepted for publication. As a service to our customers we are providing this early version of the manuscript. The manuscript will undergo copyediting, typesetting, and review of the resulting proof before it is published in its final form. Please note that during the production process errors may be discovered which could affect the content, and all legal disclaimers that apply to the journal pertain.

**The Application of Percolation Threshold Theory to Predict Compaction Behaviour of
Pharmaceutical Powder Blends**

Ana Luiza P. Queiroz¹, Waleed Faisal¹, Ken Devine², Hazel Garvie-Cook³, Sonja Vucen¹, Abina
M. Crean*¹

¹ *Synthesis and Solid State Pharmaceutical Centre, School of Pharmacy, University College
Cork, Cork, Ireland*

² *School of Pharmacy, University College Cork, Cork, Ireland*

³ *Renishaw plc, New Mills, Wotton-under-Edge, Gloucestershire, GL12 8JR, UK*

*Corresponding Author.

Tel: + 353 (21) 4901667

Email: a.crean@ucc.ie

1. INTRODUCTION

Multi-component powder blends are critical components of numerous process trains across a wide variety of manufacturing sectors. Solid dosage forms manufactured from powder blends compose a large proportion of pharmaceutical production [1]. Pharmaceutical powder blends are composed of a drug substance (active pharmaceutical ingredient) and inactive excipients to aid processing, stability and delivery [2]. Drug load is an important factor to be considered during the design of these blends. The higher the drug load, the higher the probability of the drug's properties impacting the blend's manufacturability and finished dosage form properties. For instance, Wenzel et al. showed how the increase of drug load negatively affected granulation, compression, tablet disintegration and dissolution [3]. In contrast to a gradual change in blend properties with increasing drug load, a threshold drug concentration was proposed, referred to as the percolation threshold [2]. It is proposed that issues can be expected to occur in manufacturability and drug product quality above the percolation threshold concentration of drug [2,4]. In terms of a quality by design (QbD) approach to pharmaceutical development, the percolation threshold model can aid identification of a threshold level drug above which of critical quality attributes of the formulation are undetermined. Knowing the percolation threshold drug level can aid robust formulation development by maintaining the drug below this threshold.

Percolation is a geometrical-statistical theory that includes two model types: (1) lattice model, and (2) continuum model. The lattice percolation model has been previously reported in the literature as appropriate to model tablet tensile strength for systems containing microcrystalline cellulose [5-8]. In a lattice model, percolation threshold is described the random occupation of a lattice of one substance by particles of a second

substance [5]. Consider initially a matrix of A being percolated by particles of B. As the concentration of B increases in the system, a threshold concentration will be reached and a property phase transition will be noticed. Above this threshold the system is a matrix of B percolated by particles A. The property phase transition occurs because of the formation of clumps of particle B that are connected or close enough to each other in such a way that they are linked across entire volume of the tablet, i.e. forming an infinite cluster. This theory can be extrapolated to the random distribution of a group of substances A in a lattice formed by a group of substances B [9]. In this case, the substances that form the group A need to have at least one similar property and at the same time this property must be dissimilar to the substances of group B. For example, in a tablet blend, drug substance and excipients that have poor flow could be grouped together as A, while all the substances within the formulation that have good flow would belong to group B.

Percolation threshold theory outputs a concentration range where the property analysed undergoes a sudden change, which can be observed as an edge of failure. From this theory it is possible to predict the blends that would present suboptimal properties and thereby determine an optimum drug concentration range to achieve blends designs that are robust with respect to those properties. Percolation threshold theory is mathematically described by the power law of Equation 1,

$$X = K1^*(\rho - \rho_c)^q \quad \text{Equation 1}$$

where X is one property observed (e.g. tablet strength, drug release, compactibility or electrical conductivity) [10-13]. The constant $K1^*$ is a proportionality constant or scaling factor, ρ is the occupation probability, ρ_c represents the percolation threshold and q is a critical exponent, also known as percolation coefficient.

One of the critical quality attributes to consider during the development of a tablet blend for compaction is the tablet's tensile strength. Tensile strength is defined as the resistance of a material to undergo fracture under tension [14]. It is considered a key physical property to ensure the quality of manufactured tablets. Tablets are required to have a minimum value of tensile strength to remain intact throughout downstream processing and handling. On the other hand, an increase in tensile strength can lead to an increase in the dissolution time [15]. The application of the percolation threshold model to tablet tensile strength provides valuable information in relation to blend design. The main input of this model is the tablet relative density, which replaces ρ in Equation 1. Tablet relative density is a parameter that is related to a number of individual raw material characteristics, process parameters and many subsequent tablet physical properties. The inclusion of tablet relative density makes this model a highly practical theory.

Percolation thresholds have been estimated graphically in a number of previous studies; for binary blends of MCC and mannitol [16], for binary blends at different size ratios and for different grades of HPMC blended with hydrocortisone [17], and for complex blends of mefenamic acid and a range of excipients [18]. Kuentz and Leuenberger proposed a mathematical approach in which the percolation threshold of a blend of microcrystalline cellulose (MCC) and paracetamol was modelled [8]. The authors recommended additional investigation to confirm their findings. However, there are limited publications in which the percolation threshold is predicted mathematically in the field of pharmaceutical sciences. Busignies et al. [19] showed that if the mathematical approach is selected, it is necessary to begin with modelling the percolation coefficient in order to be able to model the percolation threshold for each specific formulation, as the percolation coefficient did not seem to be universal.

The aim of this study was to define the percolation coefficient for a blend comprising MCC/ibuprofen based on a modified Heckel equation [5]. Having determined the percolation coefficient for the blend, Equation 1 was then employed to calculate the respective percolation thresholds. The blend considered contained a model drug, ibuprofen, and a commonly used excipient, MCC. These binary blend components were selected because ibuprofen exhibits poor flowability and compressibility and is prone to capping [20-22]. MCC is a widely used excipient due to its good flowability, high dilution potential and compactibility [23]. Therefore, the contrasting properties qualifies the combination of these substances as an appropriate case to apply the percolation model. Particle pore and particle shape can have significant impact on percolation threshold [24-26], therefore, two MCC grades with differing particule properties were investigated in this study: Vivapur[®] 102, an air streamed dried grade, and Emcocel[®] 90, a spray dried grade. Raman image analysis of compacted blends was employed to visually determine whether an infinite cluster of drug could be detected on the surface of tablets prepared above the percolation threshold. Properties of the powder blends and the tablets manufactured were investigated using univariate and principal component analysis (PCA) analysis to determine properties which are diminished above the percolation threshold and investigate if PCA is able to identify the critical concentration related to the percolation threshold.

2. MATERIALS AND METHODS

2.1 Materials

Microcrystalline cellulose (Vivapur[®] 102, and Emcocel[®] 90) was supplied by JRS PHARMA GmbH+Co. KG, Germany. Ibuprofen was obtained from Kemprotec Ltd., United Kingdom.

2.2 Methods

2.2.1 Powder characterization

2.2.1.1 Surface area

MCC samples were degassed for 3 h, at 120 °C and ibuprofen samples for 24 h, at 40 °C in a FlowPrep 060 sample degas system (Micromeritics, USA). The mass of each sample was between 0.4 - 0.6 g. Surface area was determined using a Gemini VI surface area and pore size analyser (Micromeritics, USA). The modelling equation applied was the Brunauer Emmett-Teller equation (BET) [27]. Liquid nitrogen at - 196 °C kept isothermal conditions and N₂ was the absorbate gas utilized. The analysis were carried out in triplicate.

2.2.1.2 Laser diffraction particle sizing

Particle size distribution was measured using a particle size analyzer (Mastersizer, Malvern Instruments, UK). A dry powder method was employed. Laser obscuration was controlled to a maximum of 5 %, and the feeding was set to a rate of 20 % for MCC and 35 % for ibuprofen, both at 1.5 bar. The height of the feeder was set to 2.5 cm. Measurements were taken for a period of 10 seconds, in triplicate.

2.2.1.3 Thermogravimetric analysis

Microcrystalline cellulose moisture content was quantified using thermogravimetric analysis (TGA) (TA Q500 TGA, TA instruments, USA). N₂ was used as the controlled atmosphere. Samples between 5 - 7 mg were loaded on the platinum pan. A ramp operation module was set up following a heating rate of 10 °C/min up to 270 °C. The weight loss measured was assumed to be moisture loss as no other thermal events occur in MCC between 0°C and 120°C as confirmed by differential scanning calorimetry (DSC).

2.2.1.4 Morphology

MCC morphology was characterized using a Malvern Morphologi G3[®] particle characterization system (Malvern Instruments, Malvern, UK). This instrument allows characterization of the shape, form and size of particles. A sample volume of 7 mm³ was automatically dry-dispersed by the Sample Dispersion Unit (SDU) which injects compressed air for 20 ms at 1 bar through the sample, onto a glass plate. A settling time of 60 seconds was held between the air injection and presentation of the sample for analysis. Malvern Morphologi G3[®] recorded individual pictures of particles and these images were acquired over 3 circular areas of the plate. The size parameters analysed were circle equivalent (CE) diameter, length and width, and the shape parameter analysed was aspect ratio. CE diameter is the correspondent diameter of a circular particle with the same area as the particle analysed. Aspect ratio is given by dividing width by length for each particle. Particles with an aspect ratio below 0.5 were classified as needle-shaped.

2.2.1.5 Scanning electron microscopy (SEM)

Scanning electron microscopy (SEM) was used to obtain images of Vivapur[®] and Emcocel[®]. A JSM-5510 SEM, (Jeol, UK) was used with heated tungsten. The morphology and particle

size of the samples were measured using an electron beam source. The voltage was constant at 3 kV. Samples were gold coated in SEM gold coater (Jeol, UK) prior to analysis to prevent charging of the samples by the SEM electron beam. A coating time of approximately 45 seconds was used to deposit a thin layer onto the samples.

2.2.2 Blend preparation

Binary blends of ibuprofen and Vivapur[®], and ibuprofen and Emcocel[®], were prepared at concentrations between 2.5 and 40 % w/w ibuprofen in MCC. A total of 300 g of each formulation was blended in Cube Mixer KB, ERWEKA (Universal Gear UG, Germany) at 30 rpm for a duration of 30 min.

2.2.3 Blend characterization

2.2.3.1 Bulk and tapped densities

Bulk and tapped densities were calculated as outlined in the European Pharmacopoeia (Ph Eur 9.0) [28]. A 100 ml cylinder was filled up to the mark with powder of a known mass, and the bulk density (ρ_{bulk}) was calculated by dividing the mass of the powder by the volume of the cylinder. The loaded cylinder was then placed in a SVM 122/222 tapped density tester, (Erweka GmbH.). The cylinder was tapped 500 and 750 times which compacted the powder by removing air from voids within the sample. The tapped density (ρ_{tapped}) was calculated by dividing the powder mass by the final volume that the powder occupied in the graduated cylinder.

2.2.3.2 True and relative densities

The true density (ρ_{true}) of materials was measured using a helium pycnometer Accupyc 1330 microprocessor controlled gas pycnometer (Micromeritics, USA). The jar volume was 11.2 cm³ and weight of the samples was 2 g. The results presented are the average of ten measurements. The relative density of powder blends (ρ_{relative}) was calculated by dividing ρ_{bulk} from Powder Flow Tester by ρ_{true} .

2.2.3.3 Flowability and compressibility

Flowability was determined by the calculation of the Hausner ratio (HR) (Equation 2) using the tapped and bulk densities determined in section 2.2.3.1 [28].

$$HR = \frac{\rho_{\text{tapped}}}{\rho_{\text{bulk}}} \quad \text{Equation 2}$$

Hausner ratio measures the loose and dense packing conditions that the powder is subjected [28, 29].

Powder flowability classification was also determined using an annular shear cell tester, Powder Flow Tester (PFT), Brookfield Engineering Laboratories, Inc., USA. This methodology is considered to be a more consistent and reliable method to determine powder flow compared to the Hausner ratio. The Hausner ratio can be variable depending on the procedure employed [29-31]. A vane lid was used in order to perform a standard flow function test. The cell volume of 43 cm³ was chosen and the mass to fill up the cell varied from 14 to 16 g across the different formulations. The major principal consolidation stresses were defined in a geometric progression that resulted in values of between 0.02 to 6.07 KPa for MCC and 0.02 and 2.98 KPa for ibuprofen. The maximum principal consolidation stresses were chosen based on earlier literature [30, 31].

Compressibility was determined for each blend using the same set up as the flowability test, however the consolidation stresses were approximately between 0.02 and 25.5 KPa and a flat lid was used. The results were expressed as bulk density vs. major principal consolidation stresses [32].

2.2.4 Direct compression

The formulations were directly compacted to form round and flat tablets with 8 mm diameter and weight of 270 ± 10 mg in a ten station rotary tablet press (Riva™ Piccola, Argentina), at a speed of 20 rpm. The relative air humidity was $50 \pm 5\%$. The compaction of each blend was performed under 14 different compaction pressures, between approximately 20 and 400 MPa. After compaction the tablets were stored for 48 hours under ambient conditions before further analysis.

2.2.5 Tablet characterization

Tablets hardness, weight, thickness and diameter were measured using a semi-automatic tablet testing system, SmartTest 50 (Sotax, Switzerland) (N=20 per blend). Tablet envelope density, (ρ_{tablet}) was obtained by dividing tablet weight by tablet volume. Tablet relative density, ρ , was calculated by dividing the tablet envelope density by the true density obtained from the annular shear cell tester for the respective powder formulation, according to Equation 3.

$$\rho = \frac{\rho_{\text{tablet}}}{\rho_{\text{true}}} \quad \text{Equation 3}$$

2.2.6 Heckel Analysis

The Heckel model was used to calculate the yield pressure, $P_{\text{yield}} = 1/(3 \cdot K)$, for each blend according to Equation 4 [33, 9]:

$$\ln\left(\frac{1}{1-\rho}\right) = K \cdot P + A \quad \text{Equation 4}$$

where ρ is the tablet relative density, P is the compaction pressure, A is a constant that represents the degree of packing that can be achieved by rearrangement of particles, i.e., before considerable inter-particle bonding take place, and K is a constant related to the ability of the powder to undergo plastic deformation.

2.2.7 Percolation coefficient and percolation threshold

Tablet tensile strength (σ_T) was calculated from measured thickness (T), diameter (D), and hardness (H) using Equation 5 [14].

$$\sigma_T = \frac{2 \cdot H}{\pi \cdot D \cdot T} \quad \text{Equation 5}$$

The percolation coefficient (T_f) when it is calculated for tensile strength was modelled using a modified Heckel equation proposed by [34]. This is given by the simplified Equation 6, in which K_2 is a constant and P is the compaction pressure.

$$\sigma_T = K_2 \cdot P^{\frac{T_f}{2}} \quad \text{Equation 6}$$

The percolation threshold, ρ_c (AB), as a critical solid fraction, was determined by the linear correlation between tablets relative density (ρ) and $\sigma_T^{\frac{1}{T_f}}$, expressed by Equation 7, for each blend [34]. The percolation coefficient (T_f) was determined by equation 6.

$$\sigma_T^{\frac{1}{T_f}} = K_3^{\frac{1}{T_f}} \cdot [\rho - \rho_c(AB)] \quad \text{Equation 7}$$

As ρ_c (AB) and $K_3^{\frac{1}{T_f}}$ are constants, Equation 7 was written as Equation 8.

$$\sigma_T^{1/T_f} = a \cdot \rho + b \quad \text{Equation 8}$$

Thus, the percolation threshold could be calculated considering the point where $\sigma_T^{1/T_f} = 0$, i.e. Equation 9.

$$\rho_c(AB) = \frac{-b}{a} \quad \text{Equation 9}$$

The values of the percolation threshold of each blend, $\rho_c(AB)$, were then used to obtain two other percolation threshold values $\rho_c(A)$ and $\rho_c(B)$ (Equation 10). While $\rho_c(B)$ represents the minimum relative density, or solid fraction, above which there is a change in tensile strength behavior, $\rho_c(A)$ is related to the dilution capacity of substance A, i.e. microcrystalline cellulose. Thus, $\rho_c(A)$ provided the fraction of ibuprofen that could be loaded into the blend with MCC in such way that MCC still leads the overall properties of the blend.

$$\rho_c(AB) = X_A \cdot \rho_c(A) + (1 - X_A) \cdot \rho_c(B) \quad \text{Equation 10}$$

A dilution capacity model was applied in order to express the $\rho_c(A)$ in terms of mass fraction (X_c), Equation 11 [8]. This conversion was performed as dilution capacity is an useful parameter to consider when designing a pharmaceutical tablet formulation.

$$X_c = -\frac{\varphi}{2} \pm \sqrt{\frac{\varphi^2}{2} - \phi} \quad \text{Equation 11}$$

In which φ and ϕ are parameters dependent of the true density of substances A (MCC) and B (ibuprofen) respectively and calculated using Equations 12 and 13 respectively.

$$\phi = \frac{\rho_{true}(A)}{\rho_{true}(A) + \rho_{true}(B)} \quad \text{Equation 12}$$

$$\phi = \frac{-2 \cdot \rho_c(A) \cdot \rho_{true}(A) - \rho_{true}(B)}{\rho_c(A) \cdot [\rho_{true}(A) + \rho_{true}(B)]} \quad \text{Equation 13}$$

2.2.8 Raman Spectroscopy

Raman imaging was carried out using a RA802 Pharmaceutical Analyser (Renishaw, UK). Placebo tablets were first analysed and reference spectra of Vivapur[®] and Emcocel[®] were generated by averaging map datasets. A reference spectrum of ibuprofen was also acquired. All tablets were measured using StreamLine[™] software package. Each tablet was measured using a 785 nm line-focussed laser to acquire approximately 76,000 spectra over an area of 8.3 mm x 8.3 mm. A measurement step size of 30 μm was used and each tablet took 15 minutes to measure. Raman images were generated using non-negative least squares (NNLS) component analysis and reference spectra for ibuprofen and the two forms of MCC.

2.2.9 Multivariate analysis

Multivariate analysis (MVA) is increasingly being used in pharmaceutical sciences [35]. Chemometrics methods, such as principal component analysis (PCA), are used to simplify data visualization, classify samples and predict variables. PCA was performed to investigate whether this technique could distinguish the behaviour of the blends below and above the percolation threshold, and, also to determine if there are differences between blends containing Vivapur[®] compared to those containing Emcocel[®]. Principal component analysis (PCA) was performed using Origin data analysis and graphing software (OriginLab, USA). The algorithm used was the singular value decomposition with full cross validation for all the blends and for the placebos of both grades of MCC. Three replicates of each blend were

input into the model. The first was the mean value of each predictor, the second is the mean minus its standard deviation and the third is the mean plus its standard deviation. The optimal number of components was three, which explained 95.51% of the variance in the total data input. The results were represented graphically by bi-plots, i.e. scores and loadings plotted in one single graphic. The scores represent the distance of each sample from the mean of all samples along each PC, therefore, blends (scores) located in close proximity are similar. The loading plot explains which variables are responsible for grouping the samples by similarity, if the grouping occurs.

3. RESULTS

3.1 Powder characterization

The particulate and bulk properties of both MCC grades and ibuprofen are summarised in Table 1. Particle size distribution determined using laser diffraction particle size analysis showed that Vivapur[®] had a slightly greater volume of particles with a larger particle size in comparison to Emcocel[®] (Figure 1a) and hence a larger D_{50} value (Table 1). A second particle size analysis method, the Morphologi G3[®] which determines particle size distribution and shape using statistical image analysis, clearly showed that the Vivapur[®] sample contained a greater percentage of particles with a larger circle equivalent (CE) diameter in comparison to Emcocel[®] (Figure 1b). Despite containing larger particles, as shown by laser diffraction particle sizing and CE, Vivapur[®] sample was also determined to have a significantly higher surface area in comparison to Emcocel[®]. An inverse relationship between particle size and surface area was not observed as MCC has a highly porous structure, as observed in the SEM images (Figure 2). According to [23] approximately 90-95% of its surface is internal,

therefore there is no relationship between particle size and surface area. A pronounced difference in the morphology between the two grades of MCC was also observed when the aspect ratio was analysed by the Morphologi G3[®]. The percentage of needle shaped particles of Vivapur[®] sample was 51%, while for Emcocel[®] sample this value was 34%. The model drug, ibuprofen, showed dissimilar properties to microcrystalline cellulose samples, exhibiting a smaller particle size distribution and surface area (Table 1, Figure 1a).

The true, bulk, tapped and relative densities of both MCC samples were similar (Table 1). Figure 3a shows that both MCC samples displayed similar powder compressibility with increase in consolidating stress. In comparison to MCC, the relative density and compressibility of ibuprofen was greater. Compressibility as a function of tapped and bulk density confirmed the findings. Both MCC grades exhibited good flowability, as expressed by Hausner ratio and flow function coefficient (Table 1). Ibuprofen was classified as cohesive when expressed by Hausner ratio and by flow function coefficient [36, 37]. Ibuprofen/MCC blends were characterized in terms of density, flow and compressibility properties (Table 2, Figure 3b, 3c). It was observed that an increase in drug content resulted in increased bulk and relative density and poorer flow properties, as indicated by the blend Hausner ratio and powder flowability classification.

3.2 Blend behaviour during tableting

Ibuprofen/MCC blends with ibuprofen content between 0 % and 30 % w/w were compacted and tensile strength calculated with respect to compaction pressure. Formulations containing 40% w/w ibuprofen/MCC could not be tableted due to poor flow from the hopper and incomplete filling of dies. Tableability profiles (Figure 4) showed that both microcrystalline cellulose grades formed tablets with high tensile strength, even at low

compaction pressures. As ibuprofen concentration was increased, a drop in tablet tensile strength was observed. Tablet weight variability, expressed as % relative standard deviation (%RSD) increased for blends with 20 % w/w ibuprofen and above (Figure 5). Increase in weight variability was attributed to a deterioration in blend flow and this behaviour is in agreement with blend flow behaviour measured for these blends (Table 2).

3.3 Percolation threshold modelling

Compaction pressures between 20 MPa to 60 MPa were selected to model percolation as the rearrangement of the particles inside the die, the phenomenon of interest, occurs at lower pressures. The modified Heckel model proposed by [34] (Equation 6) was applied for each ibuprofen/MCC blend and the respective percolation coefficient calculated (Table 3). No significant difference was observed between the percolation coefficients determined for blends prepared from Vivapur[®] and Emcocel[®] (t-value = 0.78, p-value of 0.449, p-value > 0.05). Therefore, the global mean of the individual percolation coefficients was calculated ($T_f = 3.5 \pm 0.2$) and used to determine the percolation threshold.

The linear correlation of Equation 8 is shown in Figure 6. The percolation threshold, $\rho_c(AB)$, was determined for each blend according to Equations 8 and 9, using the empirical coefficient of 3.5 (Figure 7, Table 4). The minimum relative density required to produce tablets with significant strength, $\rho_c(B)$, and solid fraction $\rho_c(A)$ related to the dilution capacity of substance A (MCC) were calculated by fitting the mass fraction of MCC. Table 5 lists the value of $\rho_c(B)$ expressed by the threshold relative density where there is a change in tensile strength behaviour. The values of $\rho_c(B)$ were 0.646 and 0.704 for blends of Emcocel[®] and of Vivapur[®], respectively. Plots of tensile strength vs. relative density of all blends were investigated and confirmed the existence of the change in tablet strength

behaviour at the predicted relative density of approx. 0.70. This behaviour is shown for selected blends in Figure 8.

Values of ρ_c were used to convert the solid fraction results into mass fraction, X_c . Finally, the critical mass fraction (X_c) was calculated from $\rho_c(A)$ using Equation 11. The X_c values obtained for Emcocel® and Vivapur® were 17.76 % w/w and 19.08 % w/w ibuprofen, respectively. The percolation thresholds and the critical mass fractions were also calculated by applying a theoretical value of percolation coefficient previously published ($T_f = 2.7$) [10] to the Equation 8. This theoretical percolation coefficient was proposed for binary mixtures in which one of the substances compacts well and the second is poorly compactable, which would apply to the ibuprofen/MCC blends. A comparison of percolation threshold values obtained using the empirical value and theoretical value is reported in Table 5.

3.4 Properties behaviour above and below the thresholds

Raman imaging showed how ibuprofen and MCC particles were distributed at the surface of the tablets (Figure 9). At drug concentrations below 15 % w/w drug the drug was distributed within a MC matrix. Significant sized clusters were observed at the concentration of 15 % w/w, however they do not form a complete pathway able to link entire surface of the tablet. At 20 % w/w a phase transition was noticed. As predicted by the percolation threshold model, there was an infinite cluster of ibuprofen particles at the surface at drug concentrations of 20 % w/w ibuprofen. The properties of the blend are majority ruled by material that forms an infinite cluster, i.e. by the ibuprofen above the threshold and by MCC below the threshold.

PCA summarised the experimental data collected during the development of the model, classified the samples into different groups, and identified the variables responsible for the variance between the samples.

Initially the data was grouped into three groups (1) *Microcrystalline cellulose*, which comprises the placebo samples, (2) *Blends Above Threshold* (concentrations of > 20 % w/w API), and (3) *Blends Below Threshold* (concentrations of < 20 % w/w API). In Figure 10a, scores of blends above the percolation threshold showed negative correlation to tensile strength (TS) loadings for all the pressures, therefore, above the threshold lower strength tablets was observed. In contrast, Hausner ratio (HR) and compressibility (Δ BD) showed a positive correlation to blends above the threshold, which means high compressibility and poor flowability. These relationships in compressibility and flowability highlighted by PCA, was also noted by univariate analysis of data (Table 2). Low porosity (P_o) at different compaction pressures and true density (TRD) showed to be highly correlated with *Blends Above Threshold*, which highlights that tensile strength was not improved with the reduction of porosity for the blends studied. The confidence interval of the groups *Blends Below Threshold* and *Blends Above Threshold* overlapped. This showed that PCA was not able to precisely predict a threshold drug concentration. Placebo samples showed a clear clustering represented by the group *Microcrystalline cellulose*. The separation of the placebo from the blends was explained mainly by the higher tensile strength and lower values of tapped (TAD), bulk (BD) and relative (RD) densities.

Figure 10b shows the second data grouping, which provides an overview of the differences between blends prepared with Vivapur[®] and blends prepared with Emcocel[®]. PC-3 differentiated these blends, to some degree (Figure 10b). There is an overlap between the groups for a selection of samples with < 10% ibuprofen loading and interestingly blends with

different grades of MCC separate from one another at higher drug loadings. This is surprising and may highlight that despite both MCC grades exhibiting similar properties, at high drug loadings their interaction with the drug differs in the blend resulting in small differences in density parameters. Overall, Emcocel® blends had slightly higher porosity and tensile strength. They also showed slightly higher tapped, relative and bulk densities, and were less compressible than those containing Vivapur®.

4. DISCUSSION

The percolation coefficient value determined in this study ($T_f = 3.5$) was higher than the theoretical coefficient ($T_f = 2.7$) published by [10]. According to [19], the percolation coefficient is dependent on the excipient and does not present a universal character. Thus, a difference between theoretical and empirical percolation coefficients was expected to occur. Other empirical strength percolation coefficients available in the literature are $T_f = 3.2$ for paracetamol and MCC (Avicel PH101) [8], $T_f = 2.1$ for Lactose, $T_f = 3.8$ microcrystalline cellulose, and magnesium stearate [19], $T_f = 4.6$ for lactose powder, and $T_f = 6.6$ for lactose granules [38], and , $T_f = 3.89$ for colloidal silica [39]. The percolation threshold coefficient has not been published for ibuprofen/MCC blends. Moreover, it was observed that other coefficients reported in the literature follow the same trend of being slightly greater than the theoretical coefficient.

In this study the percolation coefficient was modelled from compaction pressure and tensile strength, which can be easily measured. Also, the coefficient calculated could be generalised for both grades of MCC, as there was no statistically significant difference between the values calculated. This shows that the coefficient model is robust and the resulting value did

not vary for blends of the same substances, even though there may exist morphological differences (particle size and shape).

The percolation threshold determined for the binary blends with Vivapur[®] 102 and Emcocel[®] 90 differed marginally, with values of 0.1884 and 0.1718, respectively. Percolation theory explains that the threshold is a range of values close to the modelled percolation threshold, but it is not possible to determine how close [9]. Therefore, the slight difference in p_c between different MCC grades may be negligible. The critical mass fraction calculated using the theoretical coefficient resulted in higher values, 23.54 % w/w and 24.68 % w/w for blends of Emcocel[®] and of Vivapur[®], respectively. However, the flow behavior and Raman imaging showed experimentally that the threshold happens between 15 % and 20 % w/w ibuprofen. The Raman technique used gave information on the drug distribution on the tablet surface. In future studies it would be useful to consider techniques such as 3D tomographic technologies, e.g. X-ray Computational Tomography or a 3D Raman model to confirm whether the infinite cluster observed on the surface extended throughout the structure. Overall, ideally, the coefficient should be calculated for each powder blend, rather than considered as a theoretical universal value.

Blends below the critical mass fraction (≤ 15 % w/w) showed good powder flowability, which is characteristic of microcrystalline cellulose. On the other hand, blends above the critical mass fraction (≥ 20 % w/w) presented cohesive character, as the ibuprofen powder. Raman images were used to investigate ibuprofen domains in the tablets and showed for the first time ever, the visualization of the phase transition predicted for tablets using the percolation threshold model. For the blends analysed, this phase transition was observed between the mass concentrations of 15-20 % w/w, because an infinite cluster consisting of

ibuprofen domains connected to each other was observed at the concentration of 20 % w/w.

When the critical concentration has been estimated graphically [16-18], it was a retrospective methodology and had to be modelled for data from more complex analysis, e.g. dissolution. This more complex analysis would also include failure systems (above the threshold) that would need to be carried out unnecessarily. Due to advances in data processing software packages since the earlier paper [8] it is no longer challenging to model the percolation threshold mathematically. The advantage of modelling the percolation threshold mathematically is that this is a predictive tool. Flowability behaviour and tablet tensile strength could be predicted in this study based on a simple model that was only dependant on compaction pressure, tensile strength, and relative density. The other numerous characterization techniques used in this study had the aim to prove the values modelled, and investigate differences between the two different grades of MCC; they are not necessary for the percolation threshold model. Therefore, the percolation threshold model showed in this study represents a simplified mathematical predictive tool that can easily be applied for different formulations.

Principal Component Analysis was not able to identify a clear threshold level with increasing drug loading. However, PCA was able to summarize all the data collected and aided in clarifying differences between the blends according to the drug loading, and differences between the blends containing Vivapur® and the blends containing Emcocel®. Low porosity strongly and negatively correlated to blends with high drug loading which confirms that the porous regions present in the MCC placebo matrix, were occupied by particles of ibuprofen as drug in introduced. The explained variance of PC-3 (7.61 %) showed that the PCA model

only captured a small difference between Vivapur® and Emcocel® blends. The most expressive difference between these two groups along PC-3 were bulk, tapped, and relative densities, which are related to the morphological differences between both grades of MCC, captured in the SEM and Morphologi G3® analysis.

5. CONCLUSION

In this study a percolation coefficient for an ibuprofen/MCC combination was successfully modelled and the value obtained ($T_f = 3.5$) was consistent with earlier reported values for similar drug/excipient combinations. Dilution capacities of 19.08 % w/w and 17.76 % w/w ibuprofen were calculated for both Vivapur® and Emcocel® blends, respectively. A change in blend behaviour above the threshold value was confirmed by experimental flow data. Also Raman imaging confirmed the presence of infinite clusters of drug on the tablet surface above the threshold value. The minor differences in physical properties between MCC grades did not result in significantly different dilution capacities. PCA analysis of the data was not able to identify a clear threshold level with increasing drug loading. The modelling approach used in this study can be applied to early formulation development studies to identify optimal drug loading for robust pharmaceutical blend processing.

Acknowledgements

Funding: This publication has emanated from research supported in part by a research grant from Science Foundation Ireland (SFI) and is co-funded under the European Regional Development Fund [grant number 12/RC/2275].

Morphology G3 was carried out by Particular Science Ltd (Ireland), and Raman imaging analysis by Sarah Newell in Renishaw plc (UK).

ACCEPTED MANUSCRIPT

Bibliography

- [1] Järvinen, M.A., Paaso, J., Paavola, M., Leiviskä, K., Juuti, M., Muzzio, F. and Järvinen, K., 2013. Continuous direct tablet compression: effects of impeller rotation rate, total feed rate and drug content on the tablet properties and drug release. *Drug development and industrial pharmacy*, 39(11), pp.1802-1808.
- [2] Leane, M., Pitt, K., Reynolds, G. and Manufacturing Classification System (MCS) Working Group, 2015. A proposal for a drug product manufacturing classification system (MCS) for oral solid dosage forms. *Pharmaceutical development and technology*, 20(1), pp.12-21.
- [3] Wenzel, T., Stillhart, C., Kleinebudde, P. and Szepes, A., 2017. Influence of drug load on dissolution behavior of tablets containing a poorly water-soluble drug: estimation of the percolation threshold. *Drug development and industrial pharmacy*, 43(8), pp.1265-1275.
- [4] Leane, M., Pitt, K., Reynolds, G.K., Dawson, N., Ziegler, I., Szepes, A., Crean, A.M. and Dall Agnol, R., 2018. Manufacturing Classification System in the real world: factors influencing manufacturing process choices for filed commercial oral solid dosage formulations, case studies from industry and considerations for continuous processing. *Pharmaceutical development and technology*, (just-accepted), pp.1-59.
- [5] Leuenberger, H., 1999. The application of percolation theory in powder technology. *Advanced Powder Technology*, 10(4), pp.323-352.
- [6] Kozicki, J., 2007. Application of discrete models to describe the fracture process in brittle materials. Gdansk, *University of Technology*.
- [7] Kuentz, M. and Leuenberger, H., 1998. Modified Young's modulus of microcrystalline cellulose tablets and the directed continuum percolation model. *Pharmaceutical development and technology*, 3(1), pp.13-19.
- [8] Kuentz, M. and Leuenberger, H., 2000. A new theoretical approach to tablet strength of a binary mixture consisting of a well and a poorly compactable substance. *European journal of pharmaceuticals and biopharmaceutics*, 49(2), pp.151-159.
- [9] Leuenberger, H., Leu, R. and Bonny, J.D., 1992. Application of percolation theory and fractal geometry to tablet compaction. *Drug development and industrial pharmacy*, 18(6-7), pp.723-766.
- [10] Guyon, E., Roux, S. and Bergman, D.J., 1987. Critical behaviour of electric failure thresholds in percolation. *Journal de Physique*, 48(6), pp.903-904.
- [11] Fuertes, I., Miranda, A., Millán, M. and Caraballo, I., 2006. Estimation of the percolation thresholds in acyclovir hydrophilic matrix tablets. *European journal of pharmaceuticals and biopharmaceutics*, 64(3), pp.336-342.
- [12] Gonçalves-Araújo, T., Rajabi-Siahboomi, A.R. and Caraballo, I., 2008. Application of percolation theory in the study of an extended release Verapamil hydrochloride formulation. *International journal of pharmaceuticals*, 361(1-2), pp.112-117.

- [13] Hwang, K.M., Cho, C.H., Tung, N.T., Kim, J.Y., Rhee, Y.S. and Park, E.S., 2017. Release kinetics of highly porous floating tablets containing cilostazol. *European Journal of Pharmaceutics and Biopharmaceutics*, 115, pp.39-51.
- [14] Fell, J.T. and Newton, J.M., 1970. Determination of tablet strength by the diametral-compression test. *Journal of pharmaceutical sciences*, 59(5), pp.688-691.
- [15] Bi, Y.X., Sunada, H., Yonezawa, Y. and Danjo, K., 1999. Evaluation of rapidly disintegrating tablets prepared by a direct compression method. *Drug development and Industrial pharmacy*, 25(5), pp.571-581.
- [16] Pérez Gago, A. and Kleinebudde, P., 2017. MCC–mannitol mixtures after roll compaction/dry granulation: percolation thresholds for ribbon microhardness and granule size distribution. *Pharmaceutical development and technology*, 22(6), pp.764-774.
- [17] Mohamed, F.A., Roberts, M., Seton, L., Ford, J.L., Levina, M. and Rajabi-Siahboomi, A.R., 2015. The effect of HPMC particle size on the drug release rate and the percolation threshold in extended-release mini-tablets. *Drug development and industrial pharmacy*, 41(1), pp.70-78.
- [18] Kimura, G., Betz, G. and Leuenberger, H., 2007. Influence of loading volume of mefenamic acid on granules and tablet characteristics using a compaction simulator. *Pharmaceutical development and technology*, 12(6), pp.627-635.
- [19] Busignies, V., Leclerc, B., Porion, P., Evesque, P., Couarraze, G. and Tchoreloff, P., 2007. Application of percolation model to the tensile strength and the reduced modulus of elasticity of three compacted pharmaceutical excipients. *European Journal of Pharmaceutics and Biopharmaceutics*, 67(2), pp.507-514.
- [20] Nokhodchi, A., Rubinstein, M.H., Larhib, H. and Guyot, J.C., 1995. The effect of moisture on the properties of ibuprofen tablets. *International journal of pharmaceutics*, 118(2), pp.191-197.
- [21] Rasenack, N. and Müller, B.W., 2002. Crystal habit and tableting behavior. *International journal of pharmaceutics*, 244(1-2), pp.45-57.
- [22] Al-Karawi, C., Cech, T., Bang, F. and Leopold, C.S., 2018. Investigation of the tableting behavior of Ibuprofen DC 85 W. *Drug development and industrial pharmacy*, 44(8), pp.1262-1272.
- [23] Thoorens, G., Krier, F., Leclercq, B., Carlin, B. and Evrard, B., 2014. Microcrystalline cellulose, a direct compression binder in a quality by design environment—A review. *International Journal of Pharmaceutics*, 473(1-2), pp.64-72.
- [24] Lin, J. and Chen, H., 2018. Effect of particle morphologies on the percolation of particulate porous media: A study of superballs. *Powder technology*, 335, pp.388-400.
- [25] Meyer, H., Van der Schoot, P. and Schilling, T., 2015. Percolation in suspensions of polydisperse hard rods: quasi universality and finite-size effects. *The Journal of chemical physics*, 143(4), p.044901.

- [26] Nigro, B., Grimaldi, C., Ryser, P., Chatterjee, A.P. and Van Der Schoot, P., 2013. Quasiuniversal connectedness percolation of polydisperse rod systems. *Physical review letters*, 110(1), p.015701.
- [27] Brunauer, S., Emmett, P.H. and Teller, E., 1938. Adsorption of gases in multimolecular layers. *Journal of the American chemical society*, 60(2), pp.309-319.
- [28] Council of Europe. 2017. *European pharmacopoeia*. Strasbourg: European Directorate for the Quality of Medicines & HealthCare (EDQM) Council of Europe.
- [29] Santomaso, A., Lazzaro, P. and Canu, P., 2003. Powder flowability and density ratios: the impact of granules packing. *Chemical Engineering Science*, 58(13), pp.2857-2874.
- [30] Liu, L.X., Marziano, I., Bentham, A.C., Litster, J.D., White, E.T. and Howes, T., 2008. Effect of particle properties on the flowability of ibuprofen powders. *International journal of pharmaceutics*, 362(1-2), pp.109-117.
- [31] Yu, S., Gururajan, B., Reynolds, G., Roberts, R., Adams, M.J. and Wu, C.Y., 2012. A comparative study of roll compaction of free-flowing and cohesive pharmaceutical powders. *International journal of pharmaceutics*, 428(1-2), pp.39-47.
- [32] D. McGlinchey (Ed.), *Characterisation of Bulk Solids*, Blackwell Publishing, Oxford UK, 2005, pp.97-103.
- [33] Heckel, R.W., 1961. Density-pressure relationships in powder compaction. *Trans Metall Soc AIME*, 221(4), pp.671-675.
- [34] Kuentz, M. and Leuenberger, H., 1999. Pressure susceptibility of polymer tablets as a critical property: a modified Heckel equation. *Journal of pharmaceutical sciences*, 88(2), pp.174-179.
- [35] Rajalahti, T. and Kvalheim, O.M., 2011. Multivariate data analysis in pharmaceutics: a tutorial review. *International journal of pharmaceutics*, 417(1-2), pp.280-290.
- [36] Carr, R.L., 1965. Evaluating flow properties of solids. *Chem. Eng.*, 18, pp.163-168.
- [37] Thomas, J. and Schubert, H., 1979. Particle Characterization. *Partec 791979*, pp. 301–319.
- [38] Leuenberger, H. and Ineichen, L., 1997. Percolation theory and physics of compression. *European journal of pharmaceutics and biopharmaceutics*, 44(3), pp.269-272.
- [39] Ehrburger, F. and Lahaye, J., 1989. Behaviour of colloidal silicas during uniaxial compaction. *Journal de Physique*, 50(11), pp.1349-1359.

Table 1. Particulate and bulk powder properties of Vivapur[®], Emcocel[®], and ibuprofen. Average values are shown \pm standard deviation.

Property	Emcocel [®]	Vivapur [®]	Ibuprofen
D10 (μm) (n=5)	30.0 \pm 0.25	31.1 \pm 0.30	16.5 \pm 0.08
D50 (μm) (n=5)	111.6 \pm 0.73	118.0 \pm 1.60	54.9 \pm 0.21
D90 (μm) (n=5)	236.8 \pm 1.55	240.0 \pm 2.17	129.0 \pm 1.09
Surface area (m^2/g) (n=3)	1.32 \pm 0.01	1.37 \pm 0.01	0.22 \pm 0.02
True density (g/cm^3) (n=10)	1.58 \pm 0.00	1.57 \pm 0.00	1.12 \pm 0.00
Bulk density (g/cm^3) (n=3)	0.33 \pm 0.00	0.31 \pm 0.00	0.36 \pm 0.01
Relative density	0.21	0.20	0.32
Tapped density (g/cm^3) (n=3)	0.43 \pm 0.01	0.40 \pm 0.00	0.57 \pm 0.01
Hausner Ratio	1.32 (easy flowing)	1.32 (easy flowing)	1.58 (cohesive)
Flow function coefficient (n=3)	7.0 \pm 0.91 (easy flowing)	6.9 \pm 0.00 (easy flowing)	3.9 \pm 0.11 (cohesive)

Table 2. Blend density, compressibility and flow properties.

Emcocel®						
Ibuprofen (% w/w)	Bulk density (g/cm ³)	Tapped density* (g/cm ³)	True density (g/cm ³)	Relative density (g/cm ³)	Hausner Ratio	Flow character
2.5	0.34	0.43	1.52	0.22	1.26	Easy flowing
5	0.34	0.45	1.51	0.23	1.30	Easy flowing
10	0.34	0.44	1.49	0.23	1.28	Easy flowing
15	0.35	0.46	1.47	0.24	1.32	Easy flowing
20	0.35	0.47	1.45	0.24	1.36	Cohesive
30	0.35	0.49	1.38	0.25	1.39	Cohesive
Vivapur®						
Ibuprofen (% w/w)	Bulk density (g/cm ³)	Tapped density (g/cm ³)	True density (g/cm ³)	Relative density (g/cm ³)	Hausner Ratio	Flow character
2.5	0.33	0.42	1.53	0.22	1.27	Easy flowing
5	0.33	0.43	1.52	0.22	1.30	Easy flowing
10	0.33	0.43	1.48	0.22	1.30	Easy flowing
15	0.32	0.44	1.47	0.22	1.34	Easy flowing
20	0.34	0.46	1.45	0.23	1.36	Cohesive
30	0.33	0.46	1.40	0.24	1.40	Cohesive

Table 3. Percolation coefficient (Tf) values calculated for each Ibuprofen/MCC blend. r refers to Pearson's correlation coefficient.

Ibuprofen (% w/w)	Vivapur [®]		Emcocel [®]	
	Tf	r	Tf	r
0%	2.96	0.997	3.23	0.996
2.5%	3.23	0.996	3.29	0.979
5%	3.57	0.994	3.81	0.995
10%	3.52	0.996	3.80	0.996
15%	3.51	0.996	3.67	0.998
20%	3.62	0.997	3.66	0.995
30%	3.70	0.997	3.41	0.998

Table 4. Critical solid fraction, ρ_c (ab), for each blend with increase in Ibuprofen concentration. r refers to Pearson's correlation coefficient.

MCC mass fraction	Emcocel [®]		Vivapur [®]	
	ρ_c (AB)	r	ρ_c (AB)	r
1	0.1564	0.9996	0.1694	0.9999
0.975	0.2076	1.0000	0.2238	0.9999
0.95	0.2107	1.0000	0.2332	0.9999
0.9	0.2337	0.9999	0.2703	0.9999
0.85	0.2467	0.9998	0.2916	0.9997
0.8	0.2705	0.9998	0.2761	0.9992
0.7	0.3178	1.0000	0.3506	0.9997

Table 5. Comparison between theoretical [7] and empirical percolation and mass fraction parameters modelled. r refers to Pearson's correlation coefficient.

Percolation coefficient	Emcocel [®]		Vivapur [®]	
	3.5 (empirical)	2.7 (theoretical)	3.5 (empirical)	2.7 (theoretical)
pc(A)	0.180	0.267	0.200	0.288
pc(B)	0.646	0.698	0.704	0.736
r	-0.970	-0.970	-0.938	-0.934
Critical mass fraction (%)	17.76	23.54	19.08	24.68

Figure 1. Particle size distribution of Emcocel® and Vivapur® samples measured by (a) Malvern Mastersizer 3000® and (b) Morphologi G3®.

Figure 2. SEM images of (a) Vivapur® and (b) Emcocel®.

Figure 3. Plot of bulk density of (a) ibuprofen, Emcocel® and Vivapur®, blends of (b) Emcocel®, and blends of (c) Vivapur® under increasing consolidating stresses.

Figure 4. Tableability profiles of ibuprofen/MCC blends (a) Vivapur® and (b) Emcocel®. N=20, y-error bars indicate standard deviation.

Figure 5. Tablet weight variation, expressed as percent relative standard deviation (%RSD) (n=280 individual tablet weights).

Figure 6. Linear correlation between tablets relative density (ρ) and $\sigma_T \cdot T_f$, as represented by Equation 8.

Figure 7. Relationship between blends percolation threshold, $p_c(AB)$, and microcrystalline cellulose mass fraction, as represented by Equation 10.

Figure 8. Tensile strength of Vivapur®/ibuprofen blends at different relative densities. A change in tensile strength behaviour was predicted to occur in the point of intersection of two linear fits, for each blend.

Figure 9. Raman imaging of (a) Emcocel® and ibuprofen and (b) Vivapur® and ibuprofen blends. The areas in blue correspond to the excipient particles while the areas in white to API particles. The percentage express the % w/w of ibuprofen in the blend with MCC.

Figure 10. Principle component Bi-plot (scores and loadings) for (a) PC-1 vs. PC-2 and (b) PC-2 vs. PC-3, eigenvalues of 11.36, 2.71, and 1.17 for PC-1, PC-2, and PC-3, respectively. The ellipses around each group represents a 95% confidence interval. The squares represent the scores while the arrows represent the loadings.

- Modelling percolation threshold allows identification of critical drug loadings.
- A percolation coefficient $T_f = 3.5$ was determined for blends of ibuprofen and MCC.
- Calculated percolation threshold verified by testing desirable blend properties.
- Raman imaging used to visualise drug loading for formation of infinite cluster.
- Calculated percolation threshold matches drug loading to form infinite cluster.

ACCEPTED MANUSCRIPT

Abstract

Percolation theory provides a statistical model which can be used to predict the behaviour of powder blends based on particle-particle interactions. The aim of this study was to investigate if percolation theory could be used to predict the drug loading concentration of pharmaceutical tablets, and the relative density of a blend, above which tablet tensile strength is reduced, resulting in the production of unsatisfactory products. The model blend studied contained ibuprofen as the API, which exhibits poor flow and compressibility, and microcrystalline cellulose (MCC) as the excipient, which exhibits good flowability and compressibility. Two MCC grades with differing physical properties were investigated, Vivapur[®] 102 (air stream dried quality), and Emcocel[®] 90 (spray dried quality) to test the theory. Blends containing 2.5 to 40 % w/w of ibuprofen were compacted at a range of pressures and the values of the powder true density, compaction pressure, tablet envelope density, and tablet tensile strength were used to calculate the percolation thresholds mathematically. The drug loading threshold values predicted with the model (19.08% w/w and 17.76% w/w respectively for Vivapur[®] 102 and Emcocel[®] 90) were found to be in good agreement when compared to experimental data and the infinite cluster of drug was visually confirmed on the surface of tablets using Raman imaging. The capability of multivariate analysis to predict the drug loading threshold was also tested. Principal component analysis was unable to identify the threshold, but provided an overview of the changes of the analysed properties as ibuprofen drug loading increased. It was also able to identify differences between blends containing Vivapur[®] or Emcocel[®]. In conclusion, percolation theory was able to predict the maximum acceptable drug loading for this binary system of API and excipient. This methodology could be employed for other binary systems

to predict maximum drug loading potential without the need for time consuming and expensive tablet production.

ACCEPTED MANUSCRIPT

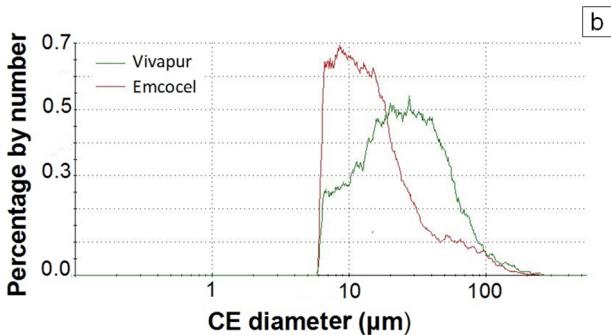
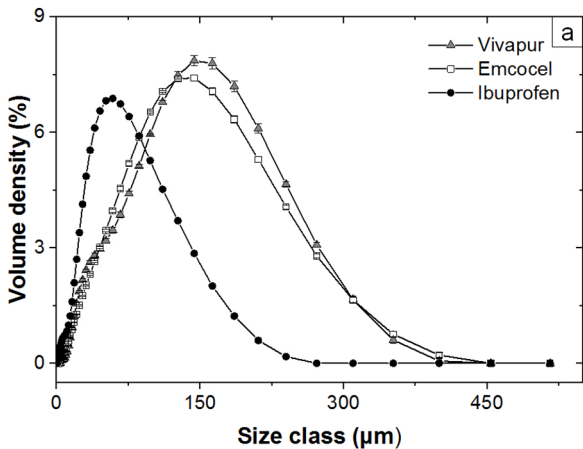


Figure 1

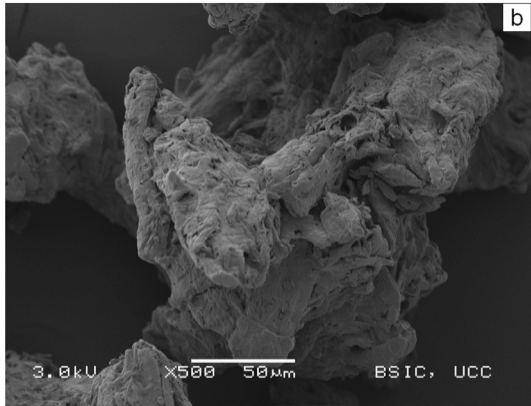
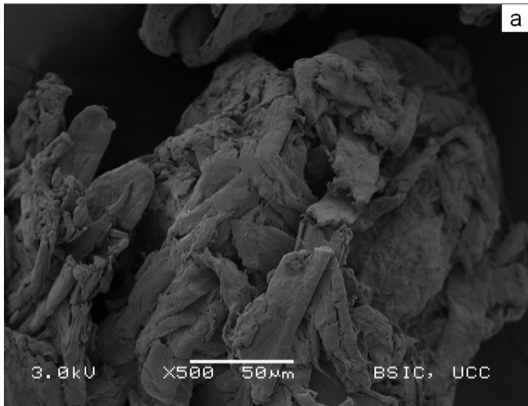


Figure 2

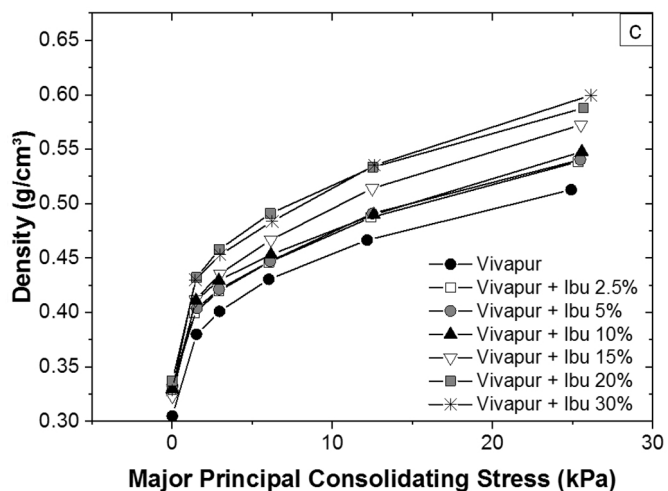
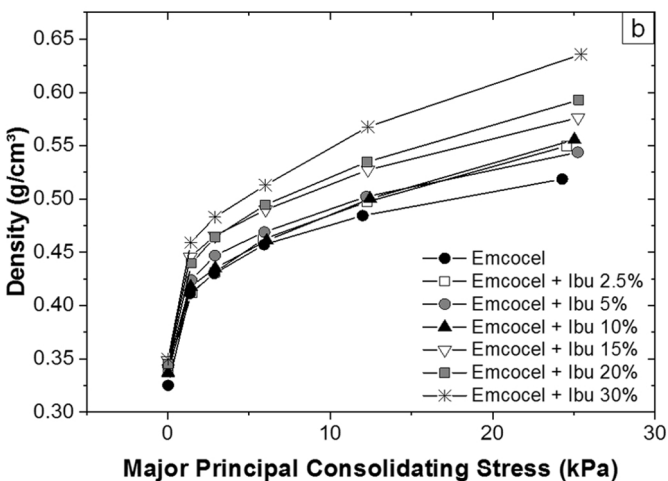
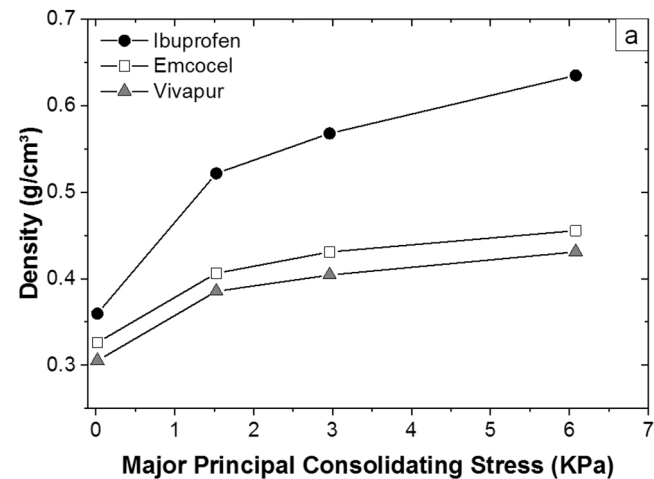


Figure 3

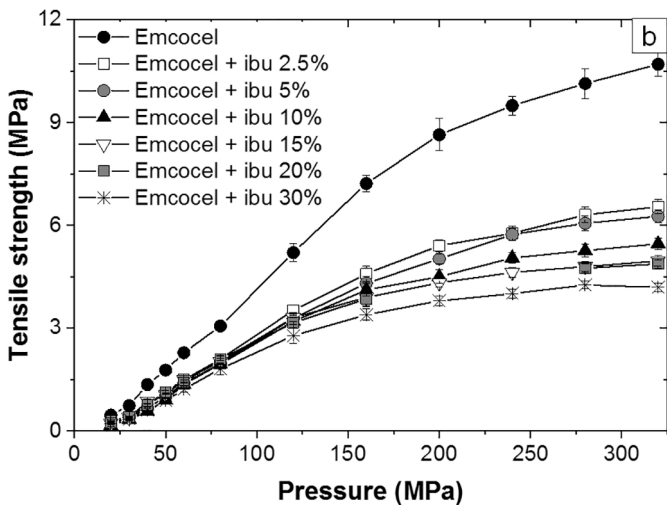
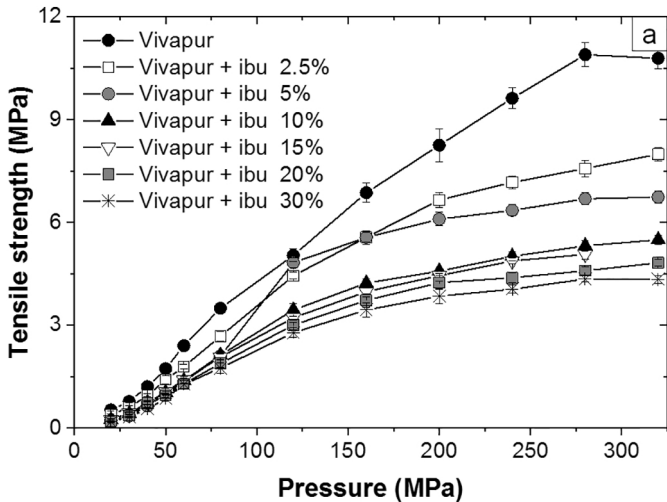


Figure 4

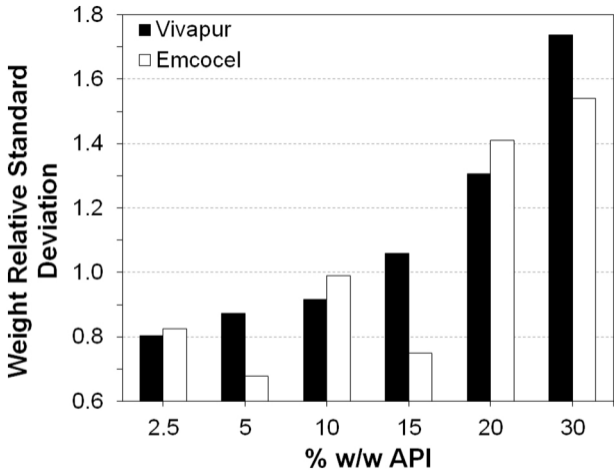


Figure 5

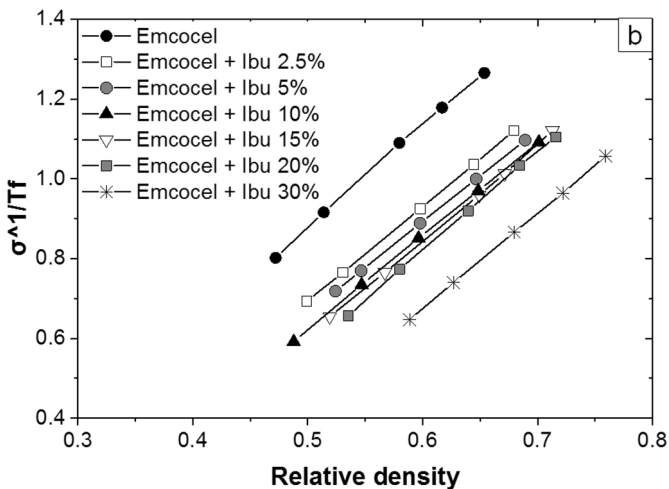
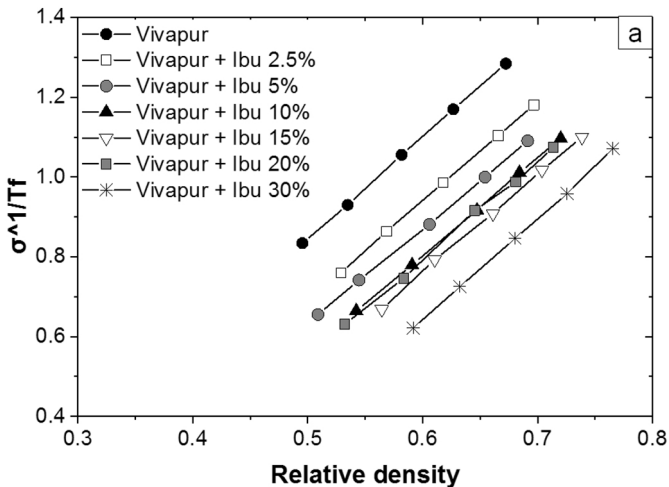


Figure 6

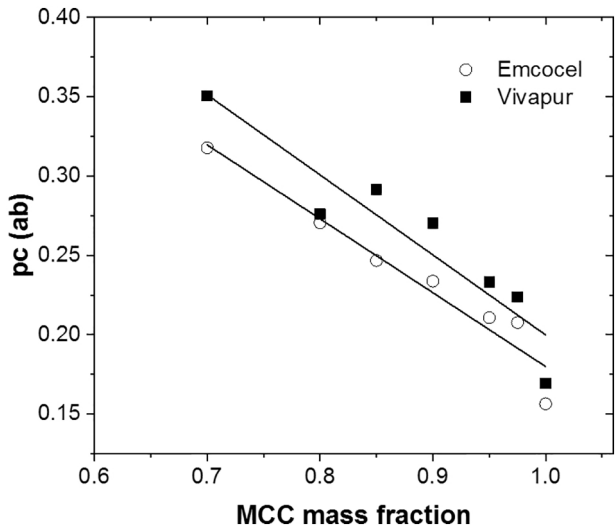


Figure 7

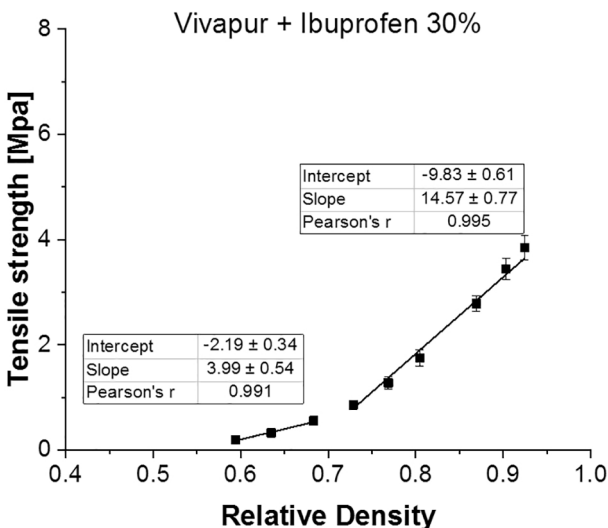
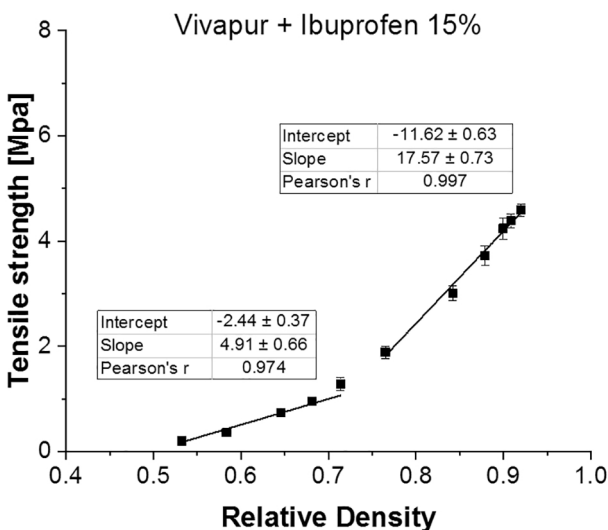
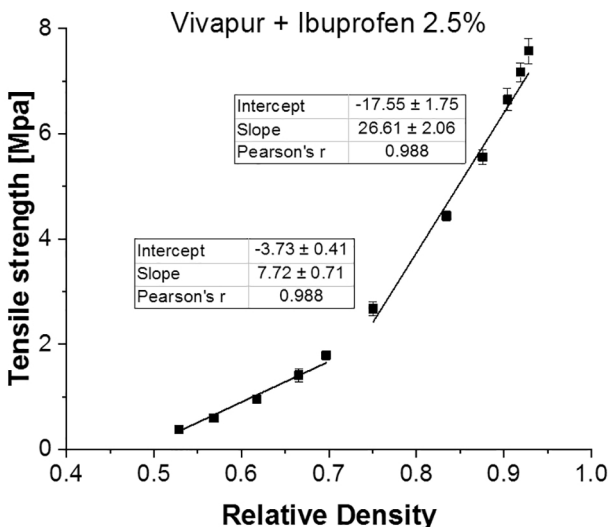


Figure 8

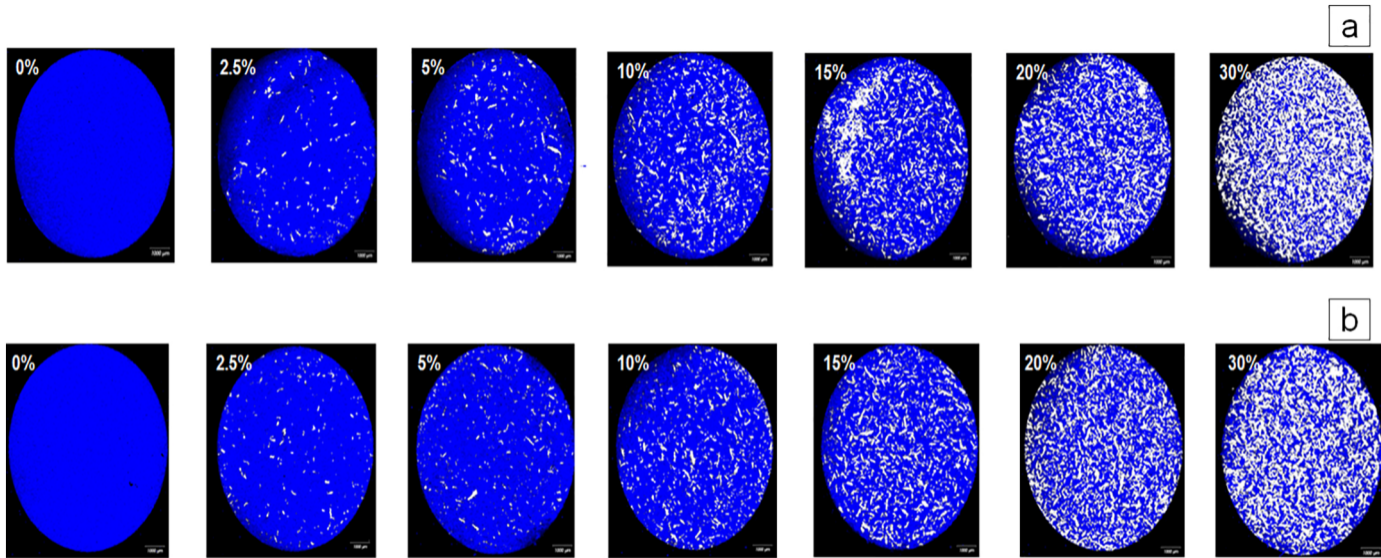


Figure 9

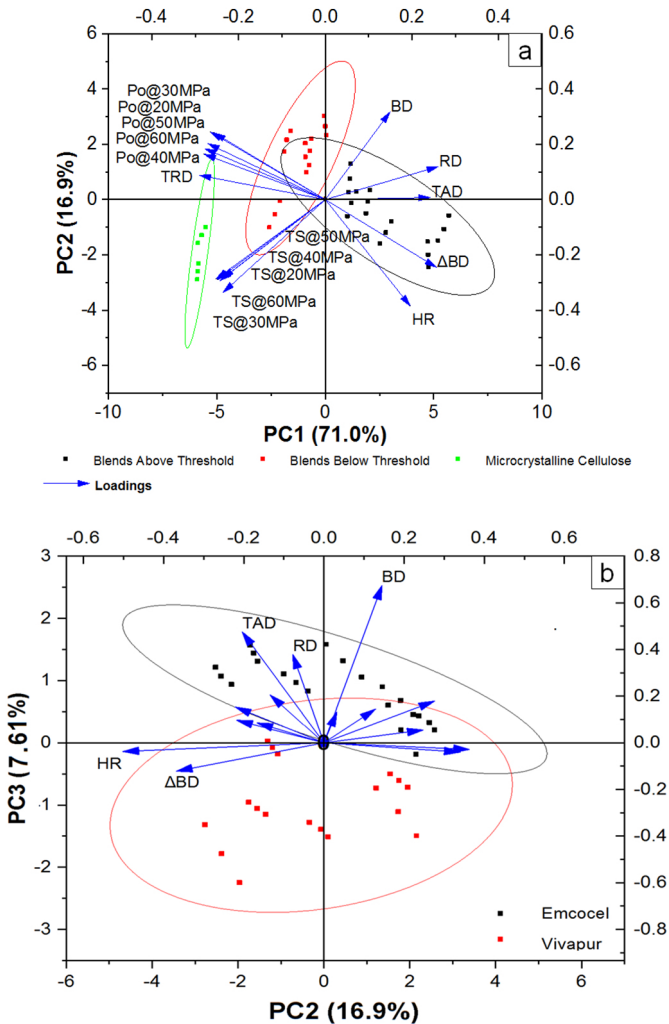


Figure 10